PHYSICAL REVIEW B **72**, 161311(R) (2005)

Electric field dependence of spin coherence in (001) GaAs/$Al_xGa_{1-x}As$ quantum wells

Wayne H. Lau*
Center for Spintronics and Quantum Computation, The University of California, Santa Barbara, California 93106, USA

Michael E. Flatté†
Department of Physics and Astronomy, The University of Iowa, Iowa City, Iowa 52242, USA

(Received 24 August 2005; published 24 October 2005)

Conduction electron spin lifetimes (T_1) and spin coherence times (T_2) are strongly modified in semiconductor quantum wells by electric fields. Quantitative calculations in GaAs/AlGaAs quantum wells at room temperature show roughly a factor of 4 enhancement in the spin lifetimes at optimal values of the electric fields. The much smaller enhancement compared to previous calculations is due to overestimates of the zero-field spin lifetime and the importance of nonlinear effects.

DOI: 10.1103/PhysRevB.72.161311 PACS number(s): 72.25.Rb, 72.25.Dc

The emerging field of semiconductor spintronics concerns the encoding, manipulation, and detection of coherence in the spin degree of freedom of mobile electrons in semiconductors.[1,2] Configuring a semiconductor material in a quantum well (QW) or other artificial structure can shorten or lengthen both the decay time of a nonequilibrium spin polarization (spin lifetime T_1) and the decay time of a coherent phase relationship between spin-up and spin-down eigenstates (spin coherence time T_2).[1,3,4] Electron spin coherence times are sensitive to carrier densities[5–7] and electric fields.[8] A series of calculations has suggested that an electric field ($\boldsymbol{\mathcal{F}}$) can dramatically lengthen spin lifetimes in (001) QWs for spins oriented along either the (110) or $(1\bar{1}0)$ directions.[9,10] Similar considerations have led to the proposal of coherent diffusive spin rotation in QWs.[11,12] These calculations rely on perturbative models of the spin precession vectors in zincblende semiconductor QWs, where the $\boldsymbol{\mathcal{F}}=0$ splittings are the sum of linear and cubic terms in the electron crystal momentum $\mathbf{K}$ and the splitting proportional to the electric field (Rashba Hamiltonian)[13,14] is also linear in $\mathbf{K}$.

Here, we report detailed calculations of spin lifetimes (T_1) and spin coherence times (T_2) in several GaAs/AlGaAs QWs at room temperature as a function of electric field. These calculations are performed using a fourteen-band electronic structure theory[15,16] which treats the spin precession vectors nonperturbatively (to all orders in $\mathbf{K}$). We find that the Rashba spin splitting deviates from a linear dependence on $\mathbf{K}$ for energies within about 100 meV of the band edge. We also find that the room-temperature electric-field-induced enhancement in the spin lifetime, for QWs between 50 Å and 150 Å, is only a factor of 4, which is much smaller than that obtained from the previous calculations based on perturbative, linear approximations.[9,10] We further find that the electron spin lifetimes and spin coherence times can be strongly influenced by an electric field, yet even for surprisingly large electric fields (<100 kV/cm), the spin decoherence is dominated by the effective internal magnetic field from the bulk inversion asymmetry. This is a very different result than has been obtained in earlier calculations that ignore the nonlinear dependence of the pseudomagnetic fields on crystal momentum.

The Hamiltonian for bulk semiconductors in the presence of an external electric field is

$$\hat{H}=\frac{\hat{\mathbf{p}}^2}{2m_e}+V(\hat{\mathbf{r}})+\frac{\hbar}{4m_e^2c^2}[\nabla V(\hat{\mathbf{r}})\times\hat{\mathbf{p}}]\cdot\hat{\boldsymbol{\sigma}}+V_{\mathrm{ext}}(\hat{\mathbf{r}}), \quad (1)$$

where m_e is the free electron mass, c is the velocity of light, e is the elementry charge, $\hat{\mathbf{p}}$ is the electron momentum operator, $V(\hat{\mathbf{r}})$ is the periodic crystal potential, $\hat{\boldsymbol{\sigma}}$ is the Pauli spin operator, and $V_{\mathrm{ext}}(\hat{\mathbf{r}})=e\boldsymbol{\mathcal{F}}\cdot\hat{\mathbf{r}}$ is the scalar potential generated by the external electric field $\boldsymbol{\mathcal{F}}$. The Schrödinger equation for heterostructure superlattices (SLs) is written as

$$\hat{H}^{\mathrm{SL}}\langle\mathbf{r}|\mathcal{L},\mathcal{S},\mathbf{K}\rangle=E_{\mathcal{LS}}(\mathbf{K})\langle\mathbf{r}|\mathcal{L},\mathcal{S},\mathbf{K}\rangle, \quad (2)$$

and the SL Hamiltonian $\hat{H}^{\mathrm{SL}}$ is given by

$$\hat{H}^{\mathrm{SL}}=\sum_{i=1}^{N_{\mathrm{layer}}}\hat{H}_i\theta_i(\mathbf{r}),\quad \theta_i(\mathbf{r})=\begin{cases}1 & \text{if } \mathbf{r}\in i\text{th layer},\\ 0 & \text{if } \mathbf{r}\notin i\text{th layer},\end{cases} \quad (3)$$

where $\hat{H}_i$ is the crystal Hamiltonian of the ith layer [Eq. (1)] with parameters tabulated in Ref. 16, N_{layer} is the number of layers in the SL unit cell, $|\mathcal{L},\mathcal{S},\mathbf{K}\rangle$ is the SL eigenstate for a carrier with wavevector $\mathbf{K}$, pseudo spin quantum number $\mathcal{S}\in\{\uparrow,\downarrow\}$, and band index $\mathcal{L}$, and $E_{\mathcal{LS}}(\mathbf{K})$ is the corresponding SL eigenenergy. To obtain $|\mathcal{L},\mathcal{S},\mathbf{K}\rangle$ and $E_{\mathcal{LS}}(\mathbf{K})$, we first solve the Schrödinger equation [Eq. (2)] at the zone center in which the SL wave vector $\mathbf{K}=\mathbf{0}$. The solution,

$$\langle\mathbf{r}|N,S,\mathbf{0}\rangle=\sum_{n\sigma}F_{NSn\sigma}(\mathbf{r})\langle\mathbf{r}|n,\sigma,\mathbf{0}\rangle, \quad (4)$$

where $|n,\sigma,\mathbf{0}\rangle$ are the corresponding zone-center Bloch states of the constituent bulk semiconductors and the expansion coefficients $F_{NSn\sigma}(\mathbf{r})$ are slowly varying envelope functions on the scale of the constituent bulk semiconductor lattice constant. The zone-center SL wavefunctions and energies are found as described in Ref. 16, Sec. III B.

Once the zone-center SL eigenstates and eigenenergies have been determinted, the SL states for $\mathbf{K}\neq\mathbf{0}$ can be obtained by application of a generalized SL $\mathbf{K}\cdot\mathbf{p}$ theory. A SL state $|\mathcal{L},\mathcal{S},\mathbf{K}\rangle$ at finite $\mathbf{K}$ is expressed in terms of the zone-

center SL states as $\langle \mathbf{r}|\mathcal{L},\mathcal{S},\mathbf{K}\rangle = \exp(i\mathbf{K}\cdot\mathbf{r})\Sigma_{NS} C_{\mathcal{L}SNS}(\mathbf{K}) \times \langle \mathbf{r}|N,S,\mathbf{0}\rangle$, where $C_{\mathcal{L}SNS}(\mathbf{K})$ are the expansion coefficients. By inserting $\langle \mathbf{r}|\mathcal{L},\mathcal{S},\mathbf{K}\rangle$ into Eq. (2), multipling the resulting equation on the left-hand side by $\exp(-\mathbf{K}\cdot\mathbf{r})\langle N,S,\mathbf{0}|\mathbf{r}\rangle$ and integrating over a SL unit cell, we have

$$\sum_{N'S'}\left[\left(\frac{\hbar^2\mathbf{K}^2}{2m_e}+E_{NS}(\mathbf{0})-E_{\mathcal{L}\mathcal{S}}(\mathbf{K})\right)\delta_{NN'}\delta_{SS'} + \frac{\hbar}{m_e}\mathbf{K}\cdot\mathbf{P}_{NSN'S'}(\mathbf{0})\right]C_{\mathcal{L}SN'S'}(\mathbf{K})=0, \quad (5)$$

where $\mathbf{P}_{NSN'S'}(\mathbf{0})\equiv\langle N,S,\mathbf{0}|\hat{\mathbf{p}}|N',S',\mathbf{0}\rangle$.

Spin splitting at finite crystal momentum in zincblende QWs occurs even without an external magnetic field due to the combined effects of spin-orbit interaction and spatial inversion asymmetry. This spatial inversion asymmetry can arise from the bulk inversion asymmetry (BIA) of the constituent semiconductors as well as the structural inversion asymmetry (SIA) of the QWs. The effect of the spin splitting on electrons can be described with an effective momentum-dependent internal magnetic field acting on the spins. If the bulk Bloch functions in Eq. (5) are inversion asymmetric (a property the fourteen-band basis preserves, but the eight-band basis does not), then both the BIA and SIA contributions to this internal magnetic field emerge naturally from solving Eq. (5) without additional assumptions. The field $\mathbf{H}(\mathcal{L},\mathbf{K})=\Upsilon^{-1/2}\mathbf{\Omega}(\mathcal{L},\mathbf{K})$, where $\Upsilon\equiv(g\mu_B\hbar^{-1})^2$, μ_B is the Bohr magneton, and g is the electron g-factor. The components of the spin precession vector $\mathbf{\Omega}(\mathcal{L},\mathbf{K})$ are given by the following relations:[16]

$$\Omega_x(\mathcal{L},\mathbf{K})=\mathrm{Re}\left[2\Omega\sum_N C^*_{\mathcal{L}\downarrow N\uparrow}(\mathbf{K})C_{\mathcal{L}\uparrow N\uparrow}(\mathbf{K})\right], \quad (6a)$$

$$\Omega_y(\mathcal{L},\mathbf{K})=\mathrm{Im}\left[2\Omega\sum_N C^*_{\mathcal{L}\downarrow N\uparrow}(\mathbf{K})C_{\mathcal{L}\uparrow N\uparrow}(\mathbf{K})\right], \quad (6b)$$

$$\Omega_z(\mathcal{L},\mathbf{K})=\sum_N \Omega[|C_{\mathcal{L}\uparrow N\uparrow}(\mathbf{K})|^2-|C_{\mathcal{L}\downarrow N\uparrow}(\mathbf{K})|^2], \quad (6c)$$

where the magnitude of the spin precession vector is given by $\Omega=\hbar^{-1}|E_{\mathcal{L}\uparrow}(\mathbf{K})-E_{\mathcal{L}\downarrow}(\mathbf{K})|$. The spin precession vector can be decomposed into $\mathbf{\Omega}(\mathcal{L},\mathbf{K})=\mathbf{\Omega}^{(D)}(\mathcal{L},\mathbf{K})+\mathbf{\Omega}^{(R)}(\mathcal{L},\mathbf{K})$ according to its symmetry, where $\mathbf{\Omega}^{(D)}(\mathcal{L},\mathbf{K})$ and $\mathbf{\Omega}^{(R)}(\mathcal{L},\mathbf{K})$ are the momentum-dependent spin precession vectors due to bulk inversion asymmetry and structural inversion asymmetry, respectively. Although many analyses of these spin splitting fields focus on the **K**-linear terms, here we keep terms to all orders.

In the linear approximations, both $[\mathbf{\Omega}_1^{(D)}(\mathcal{L},E)]^2$ and $[\mathbf{\Omega}_1^{(R)}(\mathcal{L},E)]^2$ are assumed proportional to E for all energies.[19] In addition, the nonlinear $\mathbf{\Omega}_3^{(D)}(\mathcal{L},E)$ and $\mathbf{\Omega}_3^{(R)}(\mathcal{L},E)$, are neglected in other analyses. Depending on the size of the quantum well, these two terms can become dominant. The importance of these nonlinear effects was pointed out in symmetric quantum wells.[15] Multiband calculations for asymmetric quantum wells have been done, but as a function of asymmetric doping, not as a function of an applied electric field,[17,18] and the approach used to evaluate spin lifetimes is limited to zero temperature.[18]

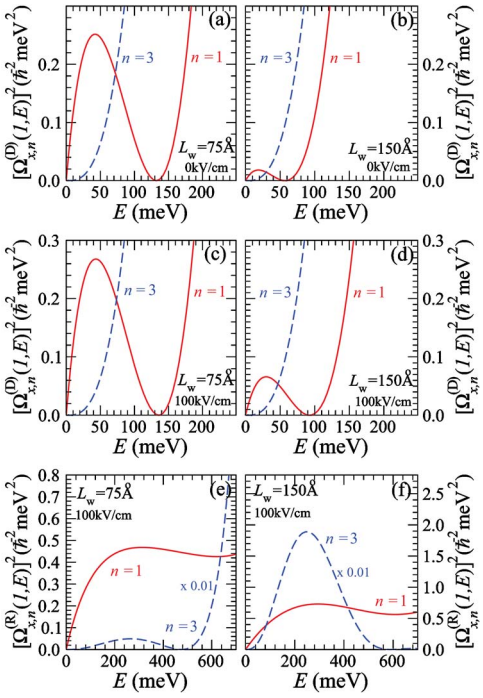

FIG. 1. (Color online) Energy dependence of electron spin precession vector for a 75 Å and a 150 Å GaAs/100 Å $Ga_{0.6}Al_{0.4}As$ QW at 300 K. $[\Omega^{(D)}_{x,n}(1,E)]^2$ as a function of E for a 75 Å QW (a), and a 150 Å QW (b) with $\mathcal{F}=0$ kV/cm. $[\Omega^{(D)}_{x,n_2}(1,E)]^2$ as a function of E for a 75 Å QW (c), and a 150 Å QW (d) with $\mathcal{F}=100$ kV/cm. $[\Omega^{(R)}_{x,n}(1,E)]^2$ as a function of E for a 75 Å QW (e), and a 150 Å QW (f) with $\mathcal{F}=100$ kV/cm.

Electron spin relaxation near room temperature is dominated by the D'yakonov-Perel' (DP) mechanism.[3,5,20] Rapid scattering from **K** to **K′** converts the **K**-dependent field of Eqs. (6) into a *time-dependent*, randomly oriented effective internal magnetic field $\mathbf{H}(\mathcal{L},E)$ that changes direction with an orbital scattering time $\tau(\mathcal{L},E)$. At any instant in time, a spin polarization decays due to random precession in the random effective magnetic field perpendicular to the spin orientation. For a precessing population, that direction is not fixed in time and it is helpful to express T_1 and T_2 in terms of the components of the random magnetic field $H_\perp(\mathcal{L},E)$ and $H_\parallel(\mathcal{L},E)$, which are transverse and longitudinal to $\mathbf{H}_o$ respectively. Thus

$$T_1^{-1}=\Upsilon\sum_{\mathcal{L}}\int dE\mathcal{D}(\mathcal{L},E)H_\perp^2(\mathcal{L},E)\tau(\mathcal{L},E)h(\mathcal{L},E), \quad (7a)$$

$$T_2^{-1}=\Upsilon\sum_{\mathcal{L}}\int dE\mathcal{D}(\mathcal{L},E)\left[\frac{1}{2}H_\perp^2(\mathcal{L},E)+H_\parallel^2(\mathcal{L},E)\right] \times\tau(\mathcal{L},E)h(\mathcal{L},E), \quad (7b)$$

where $H_\perp(\mathcal{L},E)=|\mathbf{H}(\mathcal{L},E)\times\hat{\mathbf{H}}_o|$, $H_\parallel(\mathcal{L},E)=|\mathbf{H}(\mathcal{L},E)\cdot\hat{\mathbf{H}}_o|$, $\mathcal{D}(\mathcal{L},E)$ is the density of states, and $h(\mathcal{L},E)$ is the electron distribution function.[16]

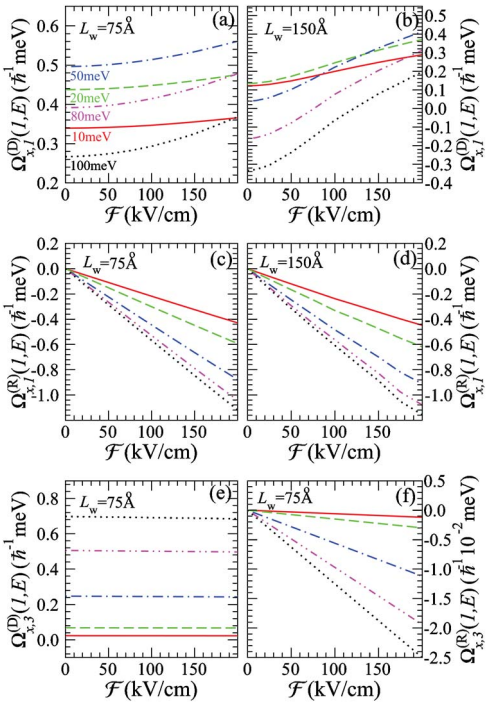

FIG. 2. (Color online) Electric field dependence of electron spin precession vector for a 75 Å and a 150 Å GaAs/100 Å $Ga_{0.6}Al_{0.4}As$ QW at 300 K. $\Omega^{(D)}_{x,1}(1,E)$ as a function of $\mathcal{F}$ for a 75 Å QW (a), and a 150 Å QW (b). $\Omega^{(R)}_{x,1}(1,E)$ as a function of $\mathcal{F}$ for a 75 Å QW (c), and a 150 Å QW (d). (e) $\Omega^{(D)}_{x,3}$ as a function of $\mathcal{F}$ for a 75 Å QW. (f) $\Omega^{(R)}_{x,3}$ as a function of $\mathcal{F}$ for a 75 Å QW.

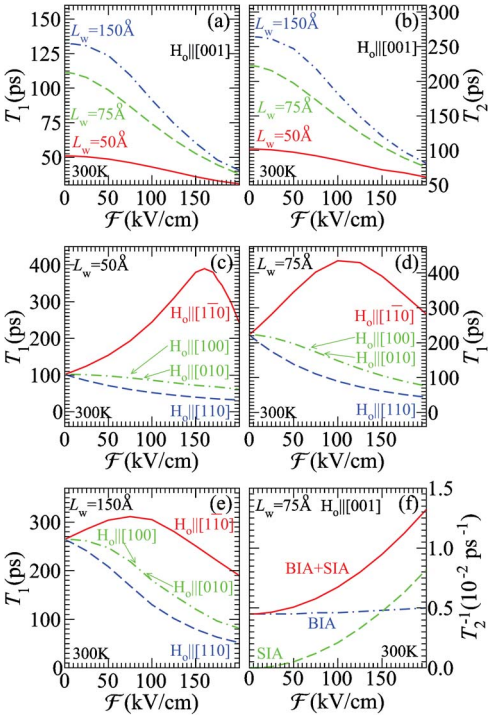

FIG. 3. (Color online) Electron spin lifetimes, coherence times, and decoherence rates as a function of applied electric field $\mathcal{F}$ for a 50 Å, a 75 Å, and a 150 Å GaAs/100 Å $Ga_{0.6}Al_{0.4}As$ QWs at 300 K with μ=800 $cm^2/V\,s$ assuming neutral impurity scattering. (a) T_1 as a function of $\mathcal{F}$ with $\mathbf{H}_o\|[001]$. (b) T_2 as a function of $\mathcal{F}$ with $\mathbf{H}_o\|[001]$. (c) T_1 as a function of $\mathcal{F}$ with $\mathbf{H}_o\|[110]$, $\mathbf{H}_o\|[1\bar{1}0]$, $\mathbf{H}_o\|[100]$, and $\mathbf{H}_o\|[010]$ for a 50 Å QW. (d) T_1 as a function of $\mathcal{F}$ with $\mathbf{H}_o\|[110]$, $\mathbf{H}_o\|[1\bar{1}0]$, $\mathbf{H}_o\|[100]$, and $\mathbf{H}_o\|[010]$ for a 75 Å QW. (e) T_1 as a function of $\mathcal{F}$ with $\mathbf{H}_o\|[110]$, $\mathbf{H}_o\|[1\bar{1}0]$, $\mathbf{H}_o\|[1\bar{1}0]$, and $\mathbf{H}_o\|[1\bar{1}0]$ for a 150 Å QW. (f) T_2^{-1} as a function of $\mathcal{F}$ with $\mathbf{H}_o\|[001]$.

Now, we present the results of our quantitative numerical calculations of the spin precession vectors, spin lifetimes, and spin coherence times of (001) GaAs/AlGaAs QWs. We find that the nonlinear effects are important and both $\mathbf{\Omega}^{(D)}_3(\mathcal{L},E)$ and $\mathbf{\Omega}^{(R)}_3(\mathcal{L},E)$ are significant in these QWs. In the absence of an external electric field, the effective internal magnetic field in a perfectly symmetric QW arises entirely from the BIA terms, and the SIA terms vanish identically. Figures 1(a) and 1(b) show $[\Omega^{(D)}_{x,n}(1,E)]^2$ as a function of energy E calculated using Eqs. (6) for a 75 Å and a 150 Å QW, respectively. $[\Omega^{(D)}_{x,1}(1,E)]^2$ is proportional to E and E^3, while $[\Omega^{(D)}_{x,3}(1,E)]^2$ is proportional to E^3, consistent with the analytical results.[3,13,14] $[\Omega^{(D)}_{x,n}(1,E)]^2$ decreases as the width L_w of the QW increases; and it deviates from a linear dependence on E within 50 meV for QWs between 50 Å and 150 Å indicating the importance of the nonlinear effects.

When an external electric field is applied along the growth direction ($\boldsymbol{\mathcal{F}}\|\hat{\mathbf{z}}$), the breaking of structural inversion symmetry results in modification of the effective internal magnetic field through both the BIA and SIA terms [Figs. 1(c)–1(f)]. $[\Omega^{(D)}_{x,1}(1,E)]^2$ increases as $\mathcal{F}$ increases, and it also increases with increasing L_w [cf., Figs. 1(a)–1(d)]. For the energy range of physical interests, $[\Omega^{(R)}_{x,1}(1,E)]^2$ is approximately two order in magnitude larger than $[\Omega^{(R)}_{x,3}(1,E)]^2$; and $[\Omega^{(R)}_{x,1}(1,E)]^2$ deviates from a linear dependence on E for energies within 100 meV [shown in Figs. 1(e) and 1(f)].

We find that the electric field dependence of $\Omega^{(R)}_{x,1}(1,E)$ is linear, whereas that of $\Omega^{(D)}_{x,1}(1,E)$ is nonlinear. The electric field dependence of $\Omega^{(D)}_{x,3}(1,E)$ is much weaker compared to that of $\Omega^{(R)}_{x,3}(1,E)$. To explore the electric field dependence of the effective internal magnetic field, $\Omega^{(D)}_{x,n}(1,E)$ and $\Omega^{(R)}_{x,n}(1,E)$ as a function of $\mathcal{F}$ are calculated for various values of E and the results for a 75 Å and a 150 Å QW are shown in Figs. 2(a)–2(f). For a constant value of E, the magnitude of $\Omega^{(D)}_{x,1}(1,E)$ and $\Omega^{(R)}_{x,1}(1,E)$ increases with increasing $\mathcal{F}$; and the slope of the curves is positive for the BIA term, while it is negative for the SIA term. The nonlinear effects are also manifested in the electric-field dependence of $\Omega^{(D)}_{x,1}(1,E)$ [see Figs. 2(a) and 2(b)]; and therefore, although cancellation of the BIA and SIA field is possible for any individual $\mathbf{K}$, cancellation of the BIA field and the SIA field for all $\mathbf{K}$ at a single electric field is not possible.

Both T_1 and T_2 are more responsive to the electric field for wide QWs [i.e. $(dT_{1,2}/d\mathcal{F})$ increases as L_w increases], and this can be seen by examining the change in $\Omega_{x,n}(1,E)$ with $\mathcal{F}$ [cf., Figs. 1(a)–1(d)]. For example, the change in $\Omega^{(D)}_{x,1}(1,E)$ from zero field to 100 kV/cm is much larger for the 150 Å QW than for the 75 Å QW. The calculations of electron spin lifetime and electron spin coherence time are

performed using Eqs. (7). To examine the electric field dependence of spin lifetime and spin coherence time with applied magnetic field along the growth direction, T_1 and T_2 as a function of $\mathcal{F}$ are calculated for a 50 Å, a 75 Å, and a 150 Å QWs at 300 K, and the results are shown in Figs. 3(a) and 3(b), respectively. For the DP mechanism, the spin lifetime, and spin coherence time are inversely proportional to the square of the effective internal magnetic field;[20] and consequently both the spin lifetime and the spin coherence time decrease with increasing electric field due to the increase of the total effective internal magnetic field with electric field.

We find that the spin-lifetime enhancement originates from the destructive interference between the BIA and SIA effective internal magnetic fields due to the symmetry breaking of structural inversion symmetry in the presence of an electric field. We also find that the calculated enhancement of the spin lifetime is much smaller than that of the previous calculations based on perturbative approaches,[10] in which the zero-field spin lifetime is overestimated and the nonlinear effects are not taken into account. To investigate the electric-field-induced enhancement in the electron spin lifetime,[9] T_1 as a function of $\mathcal{F}$ for three QWs of different thickness is calculated for an applied magnetic field parallel to the in-plane direction and the results are shown in Figs. 3(c)–3(e). As expected the calculated spin lifetime is identical for $\mathbf{H}_o \| [100]$ and $\mathbf{H}_o \| [010]$ due to the crystal symmetry of (001) QWs, and T_1 decreases with increasing $\mathcal{F}$. The electric field dependence of T_1 for $\mathbf{H}_o \| [110]$ is similar to that for $\mathbf{H}_o \| [100]$, and the spin lifetime is shorter for $\mathbf{H}_o \| [110]$ than for $\mathbf{H}_o \| [100]$. For $\mathbf{H}_o \| [1\bar{1}0]$, T_1 increases as $\mathcal{F}$ increases, reaching a maximum value ($T_1^{(\max)}$) and then it decreases as $\mathcal{F}$ further increases; i.e., BIA dominates at low field while SIA dominates at high field. $T_1^{(\max)}$ sets the upper limit for electrical tuning of spin lifetime; and $T_1^{(\max)} \to \infty$ as $\mathbf{\Omega}_n(\mathcal{L}, E) \to 0$. The spin-lifetime enhancement factor $[T_1(\mathcal{F})/T_1(0)]$ decreases as L_w increases, and the maximum enhancement factor for a 50 Å, a 75 Å, and a 150 Å QW is approximately 3.8, 2.0, and 1.2, respectively.

In the presence of an electric field, we find that spin decoherence depends on both the BIA and SIA effective internal magnetic fields, and the spin decoherence is dominated by the BIA terms at low field, while it is dominated by the SIA terms at high field. To study the effects of the BIA and the SIA effective internal magnetic fields on spin decoherence (as opposed to spin lifetimes), the decoherence rates (T_2^{-1}) as a function of $\mathcal{F}$ for a 75 Å QW due to BIA and SIA are calculated separately, and the results as well as the total decoherence rate are plotted in Fig. 3(f). It can be seen that the spin decoherence is dominated by the BIA effective internal magnetic field for an electric field as high as 100 kV/cm, and crossover occurs at approximately 150 kV/cm. The value of the crossover decreases as L_w increases, and the crossover for a 50 *Å* and a 150 *Å* QWs occurs at approximately 250 kV/cm and 120 kV/cm, respectively (not shown).

In summary, we have studied quantitatively the electric field dependence of room-temperature electron spin coherence in (001) GaAs/AlGaAs QWs using a nonpertubative 14-band electronic structure theory. We find that both the BIA and SIA effective internal magnetic fields are electric-field dependent. The electron spin lifetime and spin coherence time are strongly influenced by an electric field. Even for moderate (<100 kV/cm) electric fields, the spin decoherence is dominated by the BIA effective internal magnetic field. At optimal electric fields, the enhancement factor of spin lifetime for GaAs/AlGaAs QWs between 50 *Å* and 150 *Å* is approximately four. Finally, a technique developed by Kato *et al.*[21] can be used to observe the predicted enhanced spin lifetime, in which the in-plane spins are generated using current-induced spin polarization and the spin characteristics are probed by time-resolved Faraday or Kerr rotation.

This work was supported by DARPA/ARO.

*E-mail: wlau@mailaps.org
†E-mail: michael_flatte@mailaps.org

[1] *Semiconductor Spintronics and Quantum Computation*, edited by D. D. Awschalom, N. Samarth, and D. Loss (Springer, Berlin, 2002).
[2] S. A. Wolf *et al.*, Science **294**, 1488 (2001).
[3] M. I. D'yakonov and V. Y. Kachorovskii, Sov. Phys. Semicond. **20**, 110 (1986).
[4] Y. Ohno *et al.*, Phys. Rev. Lett. **83**, 4196 (1999).
[5] F. Meier and B. P. Zakharchenya, eds., *Optical Orientation* (North–Holland, Amsterdam, 1984).
[6] J. M. Kikkawa and D. D. Awschalom, Phys. Rev. Lett. **80**, 4313 (1998).
[7] J. S. Sandhu, A. P. Heberle, J. J. Baumberg, and J. R. A. Cleaver, Phys. Rev. Lett. **86**, 2150 (2001).
[8] O. Z. Karimov *et al.*, Phys. Rev. Lett. **91**, 246601 (2003).
[9] N. S. Averkiev and L. E. Golub, Phys. Rev. B **60**, 15582 (1999).
[10] X. Cartoixà, D. Z.-Y. Ting, and Y.-C. Chang, Appl. Phys. Lett. **83**, 1462 (2003).
[11] J. Schliemann, J. C. Egues, and D. Loss, Phys. Rev. Lett. **90**, 146801 (2003).
[12] J. C. Egues, G. Burkard, and D. Loss, Appl. Phys. Lett. **82**, 2658 (2003).
[13] E. I. Rashba, Sov. Phys. Solid State **2**, 1109 (1960).
[14] Y. A. Bychkov and E. I. Rashba, J. Phys. C **17**, 6039 (1984).
[15] W. H. Lau, J. T. Olesberg, and M. E. Flatté, Phys. Rev. B **64**, 161301(R) (2001).
[16] W. H. Lau, J. T. Olesberg, and M. E. Flatté, cond-mat/0406201.
[17] L. Wissinger, U. Rössler, R. Winkler, B. Jusserand, and D. Richards, Phys. Rev. B **58**, 15375 (1998).
[18] J. Kainz, U. Rössler, and R. Winkler, Phys. Rev. B **68**, 075322 (2003).
[19] $\mathbf{\Omega}_n(\mathcal{L}, E)$ is the Fourier coefficient of $\mathbf{\Omega}(\mathcal{L}, \mathbf{K})$ expressed as a function of energy E.
[20] M. I. D'yakonov and V. I. Perel', Sov. Phys. JETP **33**, 1053 (1971).
[21] Y. K. Kato, R. C. Myers, A. C. Gossard, and D. D. Awschalom, Phys. Rev. Lett. **93**, 176601 (2004).